algorithms

MDPI

Article

Novelty in Intelligent Controlled Oscillations in Smart Structures

Amalia Moutsopoulou [1], Markos Petousis [1,*], Georgios E. Stavroulakis [2], Anastasios Pouliezos [2] and Nectarios Vidakis [1]

[1] Department of Mechanical Engineering, Hellenic Mediterranean University Estavromenos Heraklion Crete, 71410 Iraklio, Greece; amalia@hmu.gr (A.M.); vidakis@hmu.gr (N.V.)
[2] Department of Production Engineering and Management, Technical University of Crete, Kounoupidianna, 73100 Chania, Greece; gestavr@dpem.tuc.gr (G.E.S.); tasos@dpem.tuc.gr (A.P.)
* Correspondence: markospetousis@hmu.gr; Tel.: +30-2810-379227

Abstract: Structural control techniques can be used to protect engineering structures. By computing instantaneous control forces based on the input from the observed reactions and adhering to a strong control strategy, intelligent control in structural engineering can be achieved. In this study, we employed intelligent piezoelectric patches to reduce vibrations in structures. The actuators and sensors were implemented using piezoelectric patches. We reduced structural oscillations by employing sophisticated intelligent control methods. Examples of such control methods include H-infinity and H_2. An advantage of this study is that the results are presented for both static and dynamic loading, as well as for the frequency domain. Oscillation suppression must be achieved over the entire frequency range. In this study, advanced programming was used to solve this problem and complete oscillation suppression was achieved. This study explored in detail the methods and control strategies that can be used to address the problem of oscillations. These techniques have been thoroughly described and analyzed, offering valuable insights into their effective applications. The ability to reduce oscillations has significant implications for applications that extend to various structures and systems such as airplanes, metal bridges, and large metallic structures.

Keywords: vibration; intelligent control; piezoelectric structures; H_2criterion; H-$_{infinity}$ criterion

Citation: Moutsopoulou, A.; Petousis, M.; Stavroulakis, G.E.; Pouliezos, A.; Vidakis, N. Novelty in Intelligent Controlled Oscillations in Smart Structures. *Algorithms* **2024**, *17*, 505. https://doi.org/10.3390/a17110505

Academic Editors: Sheng Du, Zixin Huang, Li Jin and Xiongbo Wan

Received: 23 September 2024
Revised: 24 October 2024
Accepted: 25 October 2024
Published: 4 November 2024

1. Introduction

In this study, a smart engineering structure was used for vibration suppression. Vibration suppression in smart structures involves the use of advanced materials and technologies to control and reduce unwanted vibrations for various engineering applications [1–8]. Smart structures integrate actuators, sensors, and control algorithms to adapt to varying conditions and improve performance. The following are the key aspects of vibration suppression in smart structures. Smart materials play a crucial role in the suppression of vibrations. Piezoelectric materials are a common type of smart material. When these materials are subjected to mechanical stress, they generate electric charge [2–7]. They are capable of serving as actuators as well as sensors, converting mechanical vibrations into electrical signals and vice versa.

Several researchers have used piezoelectric smart structures to suppress vibration [7–13]. Smart structures utilize piezoelectric actuators and sensors. Piezoelectric actuators have revolutionized smart engineering structures by providing precise, responsive, and efficient control mechanisms [14–17]. Their applications across various fields, from aerospace and civil engineering to robotics and optics, demonstrate their versatility and effectiveness. Despite some challenges related to material limitations and costs, ongoing research and technological advancements have been poised to overcome these hurdles, paving the way for broader adoption and new innovations in smart engineering structures. The application of piezoelectric materials as actuators in intelligent engineering structures is a rapidly

growing field driven by the unique properties of piezoelectric materials and their ability to perform precise and responsive control functions [18–22]. An in-depth analysis of this subject shows that piezoelectric actuators leverage direct and inverse piezoelectric effects, converting electrical energy into mechanical motion, and vice versa. This enables them to function as both sensors and actuators. Piezoelectric actuators can be very small and lightweight, which is beneficial for applications where weight and space are critical, such as in aerospace and medical devices [23–27].

In this study, piezoelectric materials were used as actuators and sensors. We employed co-localized actuator pairs implanted in laminated composite beams (piezoceramic PZT G-1195N, with a Young's modulus Ep of 6.3×10^{10} N/m^2) composed of graphite/epoxy, glass/epoxy, and metallic (aluminum) beams. Advanced materials and systems, termed as smart piezoelectric structures, utilize the distinctive characteristics of piezoelectric materials to provide intelligent, adaptive, and frequent self-monitoring capabilities. Piezoelectricity denotes the capacity of a material to generate an electrical charge when subjected to mechanical stress. However, these materials may be distorted when an electric field is applied. The use of smart materials is a key component of vibration suppression in smart structures. Piezoelectric materials are among the most commonly used smart materials. These materials possess a distinctive capability to generate an electric charge when subjected to mechanical stress [6–11]. This property enables them to function as actuators and sensors capable of converting mechanical vibrations into electrical signals, and vice versa.

Numerous researchers have explored the use of piezoelectric smart structures for suppressing vibrations [7–17,28]. The integration of piezoelectric actuators and sensors into smart structures has been transformative, offering precise, responsive, and efficient control mechanisms, which have significantly advanced the capabilities of smart engineering structures [14–20,28].

This work can make an important contribution to engineers who want to apply new smart materials with appropriate control techniques that can contribute to the reduction in oscillations [6,7,29–31]. In the field of both civil and mechanical engineering, an important problem is the reduction in oscillations created by dynamic loads, such as earthquakes and wind. The methods and control techniques used were described in detail in [32]. This work has important applications because the problem of reducing oscillations is a common problem for both civil and mechanical engineers [32]. These applications can be used in airplanes, metal bridges, and large metal structures. Structures are stressed by dynamic loads such as wind and earthquake loading [32]. This paper outlines and explains the various methods and control techniques used to address this issue. This research is highly relevant because it addresses the shared challenge of oscillation. The applications of the outlined methods are broad, potentially benefiting areas such as airplane design, metal bridges, and large metal structures, all of which are subjected to dynamic stresses from wind and seismic activity. The development of effective strategies to control these vibrations is essential for the stability and durability of these structures.

When materials are subjected to an electric field, they can experience distortion, a phenomenon that holds significance for engineers working on the development and application of advanced smart materials. By employing appropriate control techniques, these smart materials can play a vital role in minimizing oscillations, which is a crucial concern in various engineering fields. This issue is especially relevant for both civil and mechanical engineers, who frequently grapple with the challenge of reducing vibrations caused by dynamic forces such as earthquakes and wind.

These structures are often exposed to dynamic loading conditions, including those imposed by wind and seismic activity, which can induce vibrations that compromise their stability and integrity. Therefore, it is essential to develop and implement effective control techniques for reducing vibration. The findings of this study could lead to advancements in the design and maintenance of structures that are more resilient to dynamic stresses, ultimately enhancing their safety, performance, and longevity. This study plays a crucial role in advancing the reduction in oscillations, which is an area of significant concern

in engineering. This research begins with a comprehensive modeling process utilizing the finite element method as the foundational approach. The equations used for this modeling are meticulously detailed, specifically in Equations (1)–(10), providing a thorough understanding of the application of the finite element method in this context.

Subsequently, this study introduces equations pertinent to control theory, which is an essential aspect of managing and reducing oscillations. A key focus is placed on the derivation of the transfer function, which is fundamental in control theory to understand how systems respond to various inputs. This derivation is presented in detail to ensure clarity in the development and application of the transfer function.

The analysis within the study was multifaceted, employing both state–space domain and frequency domain analyses. The state–space domain analysis is elaborated upon through Equations (10) to (14), offering insights into the system's behavior in the time domain representation. Additionally, frequency domain analysis is thoroughly explored in Equations (15)–(33), providing an in-depth examination of how the system responds to different frequencies. By combining these analytical approaches, this study offers a comprehensive strategy to address and mitigate oscillations in various engineering applications.

2. Motion Formula of the Smart Structure

The beam formula for both mechanical and electrical loads is calculated by [7,17–19,28,33]:

$$EI\frac{\partial^4 y(t,x)}{\partial x^4} + \rho bAb\frac{\partial^2 y(t,x)}{\partial t^2} = f_m(t,x) + f_e(t,x) \quad (1)$$

E is Young's modulus, I is the moment of inertia, p is density, A is area, f_e is the electrical force, and f_m is the disturbance (mechanical force) [33].

Figures 1 and 2 depict a smart beam incorporating an embedded piezoelectric actuator that produces a mechanical load in the form of a force when subjected to an electrical current [6,7]. Figure 1 shows a smart beam with embedded actuators.

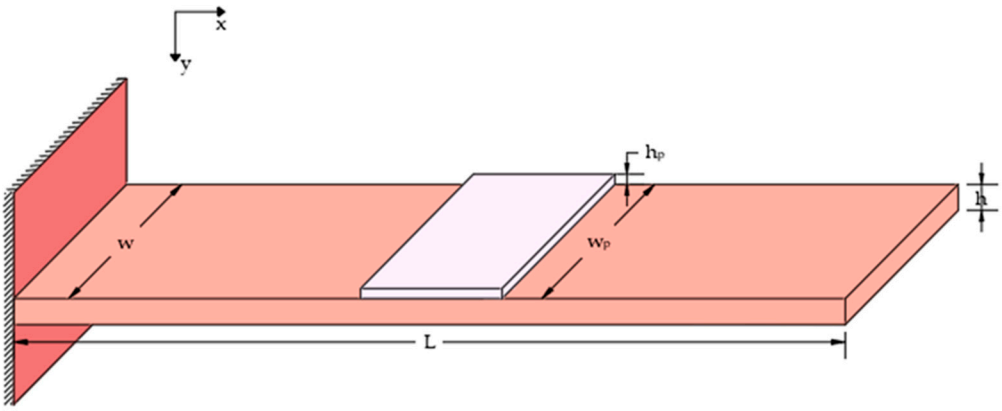

Figure 1. Piezoelectric patch attached to a beam.

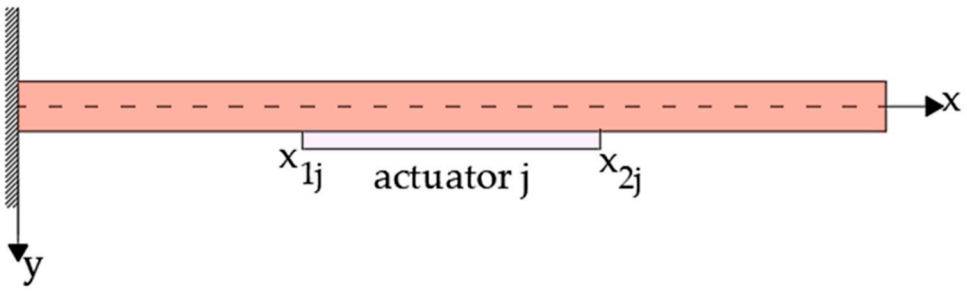

Figure 2. One pair of actuator patches.

Figure 2 shows the actuator integrated into the beam. This figure shows the ends of the actuator used in further equations, which are very important for the electrical matrices of our system. All modeling is based on Equation (1) [33]; from the solution of this equation, the results are given in the time domain. The results without control are given by applying the differential, whereas the results with control are given after the application of the infinity control.

To determine the electric force generated by the piezoelectric actuator $f_e(t,x)$, the following equation was used:

$$f_e(t,x) = \frac{\partial^2 M_{px}(t,x)}{\partial x^2} \tag{2}$$

where M_{px} is the piezoelectric actuator's bending moment.

Where Pzt (piezoelectric patch) placed on the beam is indicated by the step function H. The bending moment M_{px} is given by

$$M_{px}(t,x) = C_0 e_{pe}(t)\left[H\left(x - x_{1j}\right) - H\left(x - x_{2j}\right)\right]u_j(t) \tag{3}$$

This equation is derived from the theory of piezoelectric materials, where [16,17]

$$C_0 = EI \cdot K_f \tag{4}$$

$$K_f = \frac{12EE_p hh_p\left(2h + h_{p)}\right.}{16E^2h^4 + EE_p\left(32h^3h_p + 24h^2h_p^2 + 8hh_p^3\right) + E_p^2h_p^4} \tag{5}$$

The piezoelectric patch mechanical tension $e_{pe}(t)$ is derived by

$$e_{pe}(t) = \frac{d_{31}}{h_p}u_j(t) \tag{6}$$

The constant d_{31} combines the electric intensity $e_{pe}(t)$ with the electric voltage $u_j(t)$, which is generated in an actuator j (Figure 2). Where d_{31} is the piezoelectric constant d31 = 280×10^{-12} m/V (Table 1).

Table 1. Smart beam specifications (graphite/epoxy T300/976).

Specifications of the Beam	Value
L stands for length	1.40 m
W stands for the width	0.07 m
h is height	0.02 m
ρ represents the density	1700 kg/m^3
E is the Young's modulus	1.8×10^{11} N/m^2
Pzt thickness is bs and ba	0.003 m
d31 is the electrical conductivity	280×10^{-12} m/V

Thus, Function (3) can be expressed as a flexural moment as follows:

$$M_{px}(t,x) = C_p\left[H\left(x - x_{1j}\right) - H\left(x - x_{2j}\right)\right]u_j(t) \tag{7}$$

where

$$C_p = EIK_f\frac{d_{31}}{h_p}$$

The electric force is obtained as follows using Equations (2) and (3):

$$f_e(t,x) = C_p u_{aj}(t)\left[\delta'(x - \text{x1j}) - \delta'(x - \text{x2j})\right] \tag{8}$$

The following function, which depicts the smart beam's response to the dynamic (electrical) force generated by the piezoelectric patch and the lateral dynamic disturbance, was derived using Equations (1) and (8):

$$EI\frac{\partial^4 y(t,x)}{\partial x^4} + \rho bAb\frac{\partial^2 y(t,x)}{\partial t^2} = q_0(t) + C_p u_j(t)[\delta'(x - x_{1j}) - \delta'(x - x_{2j})] \tag{9}$$

In the case of j-equivalent piezoelectrics (Figure 3), Equation (9) becomes

$$EI\frac{\partial^4 y(t,x)}{\partial x^4} + \rho bAb\frac{\partial^2 y(t,x)}{\partial t^2} = q_0(t) + C_p u_j(t)\sum_{i=1}^{j}\left[\delta'(x - r_{1j}) - \delta'(x - x_{2j})\right]$$

where δ′(x) is the derivative of the Dirac function with respect to its independent variable.

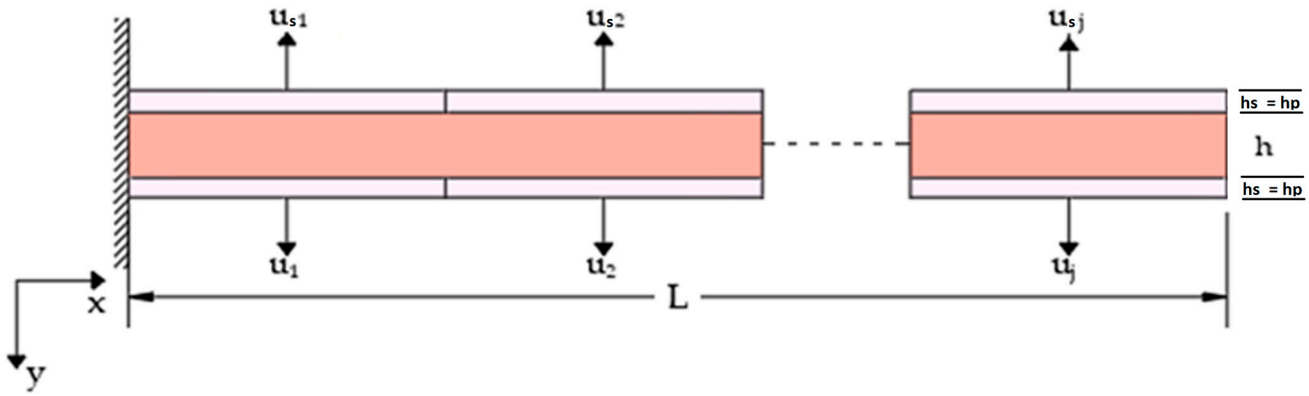

Figure 3. An intelligent beam that incorporates piezoelectric actuators and sensors.

From the solution of the partial differential equations of the beam, we pass to the finite element method, which transforms the system of the beam into a system of ordinary differential equations. The solution of the finite elements converges with the solution of the partial differential equation by increasing the number of elements. In the next chapter, the tables of the damping stiffness mass matrices and electrical matrix used for the modeling, as calculated by the authors, are used [1,33,34].

2.1. Modelling

In this work, the Eyler–Bernoulli beam equation (Equation (1)) is used, by integrating this equation and using a Hermite multivariable, the local matrices are derived for the mass, stiffness, and damping electric charge matrices of the structure. Assembling is then performed on the global stiffness model. A reference related to the finite element method is given [1,33]. In our analysis, we use two degrees of freedom in the finite element method—the transport deflection ψ and the rotation. In addition, we use two different disturbances, one static and one dynamic.

The goal of this study was to reduce oscillations using intricate control techniques and piezoelectric materials. In particular, the locations of piezoelectric actuators were defined. Figure 4 shows the actuators positioned at each of the four points (labels 1, 2, 3, and 4) along the beam. The dynamical description of the system is given by [1,35]

$$\text{M}\ddot{q}(t) + \text{D}\dot{q}(t) + \text{Kq(t)} = \text{fm(t)} + \text{fe(t)} \tag{10}$$

where fe represents the results of the electromechanical coupling affecting the global control force vector, D is the viscous damping matrix, K is the global stiffness matrix, and M is

the global mass matrix. fm is the mechanical vector of the global external loading and fe is the electrical vector. The independent variable is a vector q(t) composed of transversal deflections ψ_i and rotations w_i, or

$$q(t) = \begin{bmatrix} w_1 \\ \psi_1 \\ \vdots \\ w_n \\ \psi_n \end{bmatrix} \tag{11}$$

where n denotes the finite element number employed in the analysis [7]. As is common practice, we switch the representation to a state–space control form [9–15].

$$\begin{aligned} x(t) &= \begin{bmatrix} q(t) \\ \dot{q}(t) \end{bmatrix} \\ &= \begin{bmatrix} 0_{2nxn} \\ M^{-1}(f_m(t) + f_e(t) \end{bmatrix} + \begin{bmatrix} \dot{q}(t) \\ -M^{-1}D\dot{q}(t) - M^{-1}Kq(t) \end{bmatrix} \\ &= \begin{bmatrix} 0_{2nxn} \\ M^{-1}(f_m + f_e)(t) \end{bmatrix} + \begin{bmatrix} 0_{2nx2n} & I_{2nx2n} \\ -M^{-1}K & -M^{-1}D \end{bmatrix} \begin{bmatrix} q(t) \\ \dot{q}(t) \end{bmatrix} \\ &= \begin{bmatrix} 0_{2nxn} \\ M^{-1}f_m(t) \end{bmatrix} + \begin{bmatrix} 0_{2nxn} \\ M^{-1}f_e(t) \end{bmatrix} + \begin{bmatrix} 0_{2nx2n} & I_{2nx2n} \\ -M^{-1}K & -M^{-1}D \end{bmatrix} \begin{bmatrix} q(t) \\ \dot{q}(t) \end{bmatrix} \end{aligned} \tag{12}$$

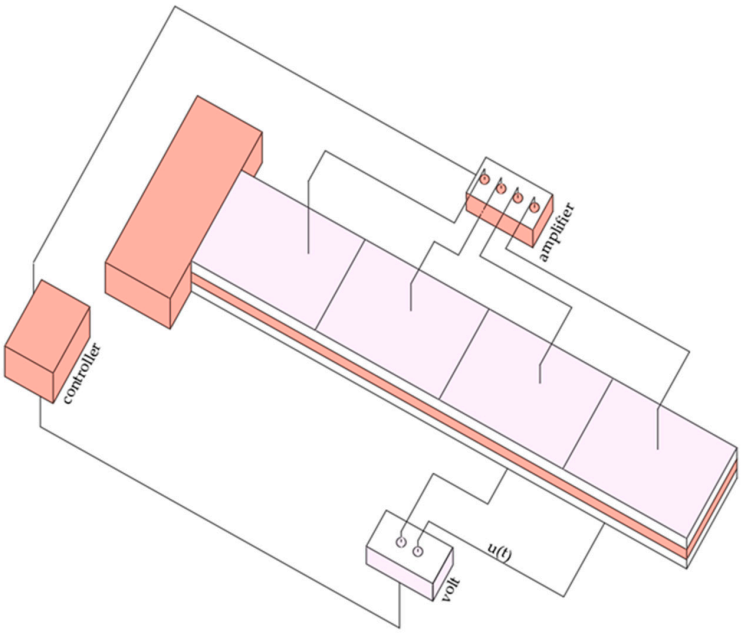

Figure 4. The actuators were positioned over the entire smart structure.

Additionally, the value $f_e(t)$ is denoted as where the unit's piezoelectric force (of size $2n \times n$) is when it is placed on the proper actuator.

$$Fe(t) = \begin{bmatrix} 0 & 0 & 0 & 0 \\ cp & -cp & 0 & 0 \\ 0 & 0 & 0 & 0 \\ 0 & cp & -cp & 0 \\ 0 & 0 & 0 & 0 \\ 0 & 0 & cp & -cp \\ 0 & 0 & 0 & 0 \\ 0 & 0 & 0 & cp \end{bmatrix} \tag{13}$$

where u denotes the actuator voltage. The disturbance vector is denoted as $d(t) = f_m(t)$. Then,

$$\begin{aligned}\dot{x}(t) = \begin{bmatrix} 0_{2n\times 2n} & I_{2n\times 2n} \\ -M^{-1}K & -M^{-1}D \end{bmatrix} x(t) + \begin{bmatrix} 0_{2n\times n} \\ M^{-1}F_e^* \end{bmatrix} u(t) + \begin{bmatrix} 0_{2n\times 2n} \\ M^{-1} \end{bmatrix} d(t) \\ = Ax(t) + Bu(t) + Gd(t) \\ = Ax(t) + [BG] \begin{bmatrix} u(t) \\ d(t) \end{bmatrix} \\ = Ax(t) + \widetilde{B}\widetilde{u}(t),\end{aligned} \tag{14}$$

The output function (displacement measured alone) can be used to enhance this result.

$$y(t) = [x1(t)\ x3(t) \ldots xn - 1(t)]T = C\ x(t)$$

where

$$C = [1\ 0\ 0 \ldots .0; -1\ 0\ 1\ 0 \ldots .0; 0\ 0 -1\ 0\ 1 \ldots .0; 0\ 0\ 0\ 0 -1\ 0\ 1 \ldots .0]$$

The ability to convert mechanical stress into strain, and vice versa, is a feature of the piezoelectric effect. The reduction in oscillations attained in this study is based on this. Actuator pairs co-localized with piezoceramics (PZT G-1195) were employed in our simulation for laminated composite beams made of graphite/epoxy, aluminum, and glass/epoxy (Figure 5). Table 1 lists the specifications of the smart beams.

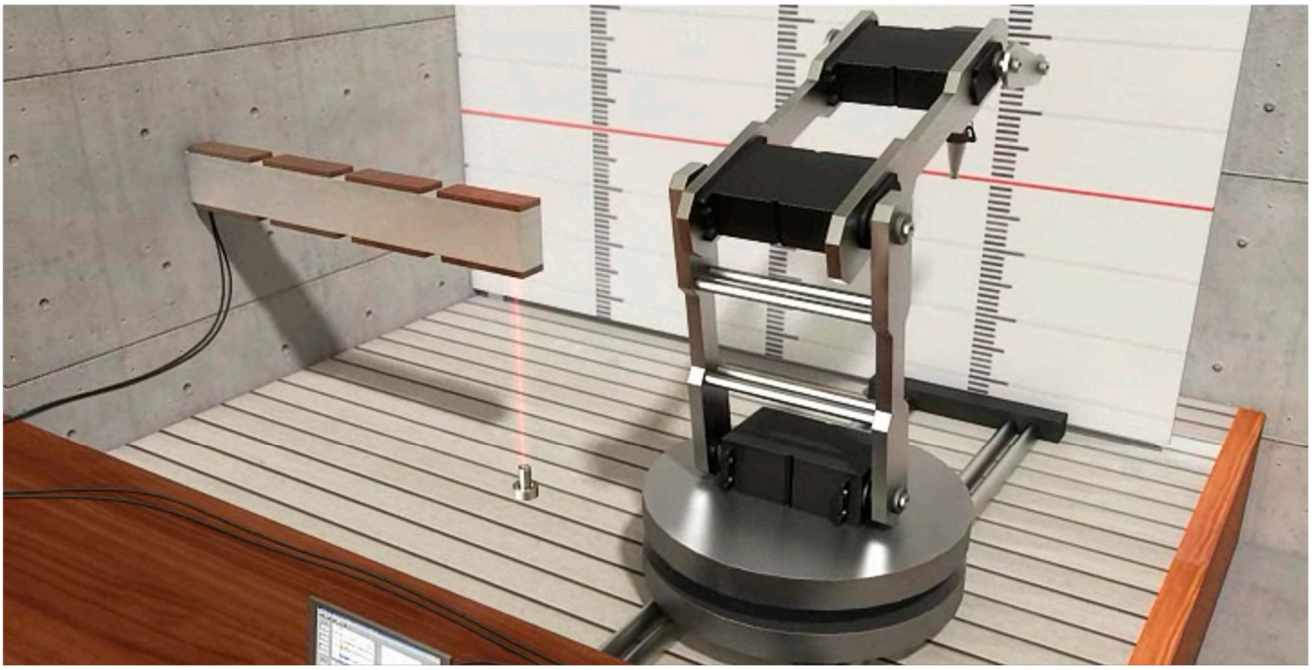

Figure 5. Smart structure.

2.2. Connection to the Issue of Beam Control

The given problem involves taking the disturbance (d) and measurement noise (n) as inputs and producing displacement measurements (y) and controller voltages (u) as the outputs. The provided structural diagrams and equations were employed to simulate this particular issue involving a beam and were implemented using MATLAB v. 5.0. In the frequency domain, the objective is to determine the optimal transfer function N. To achieve this, it is beneficial to derive the input-output relationships for the initial model [16,21].

$$\begin{bmatrix} u \\ e \end{bmatrix} = F(s) \begin{bmatrix} d \\ n \end{bmatrix} \Rightarrow z = F(s)w$$

as illustrated in Figure 5.

In Figure 6, K(s) is the controller, d is the disturbance, e is the error, n is the noise, u is the control voltage, and x is the state vector.

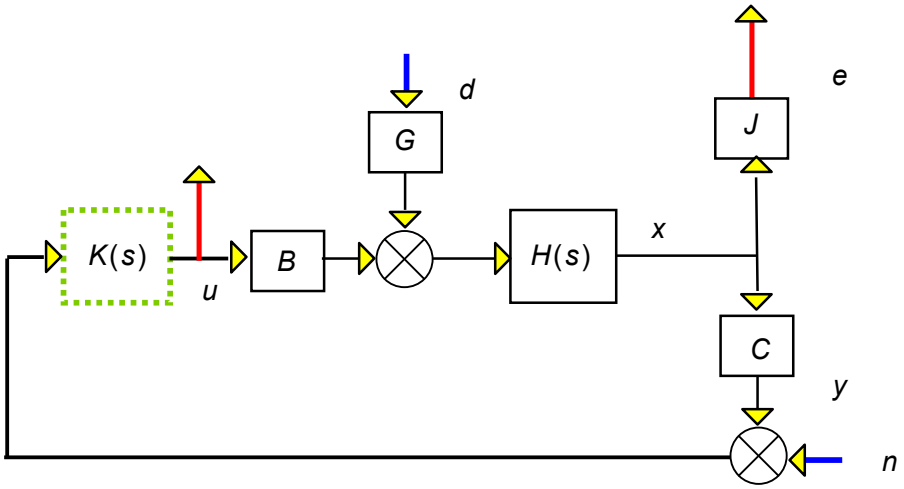

Figure 6. Beam with noise output, error, disturbance input, and controller.

Where the beam is explained by [31]

$$\dot{x}(t) = Ax(t) + [B\ G] \begin{bmatrix} u(t) \\ d(t) \end{bmatrix}$$

In the frequency domain, the transfer function H(s) is

$$H(s) = (sI - A)^{-1} \tag{15}$$

J is used to select the states that we aim to control, which may differ from y. In most studies, J is

$$J = \begin{bmatrix} 1 & 0 & 0 & 0 & 0 & 0 & 0 & 0 & 0 & 0 & 0 & 0 & 0 & 0 & 0 & 0 \\ 0 & 0 & 1 & 0 & 0 & 0 & 0 & 0 & 0 & 0 & 0 & 0 & 0 & 0 & 0 & 0 \\ 0 & 0 & 0 & 0 & 1 & 0 & 0 & 0 & 0 & 0 & 0 & 0 & 0 & 0 & 0 & 0 \\ 0 & 0 & 0 & 0 & 0 & 0 & 1 & 0 & 0 & 0 & 0 & 0 & 0 & 0 & 0 & 0 \end{bmatrix} \tag{16}$$

We commenced by gradually re-performing Figure 6.

It is clear from Figure 7 that the disruption to the inaccuracy in the transfer function is

$$T_{de} = J \cdot (I - HBKC)^{-1} H \cdot G \tag{17}$$

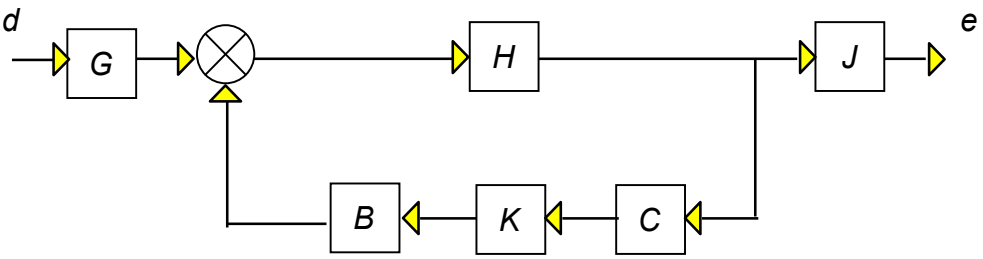

Figure 7. Block diagram disturbance and errors.

Equation (17) is a frequency domain equation, and an attempt was made to derive the transfer function Tde that relates the external disturbance to the error.

It is evident from Figure 8 that the noise-to-error transfer function is

$$T_{ne} = J \cdot (I - HBKC)^{-1} HBK \tag{18}$$

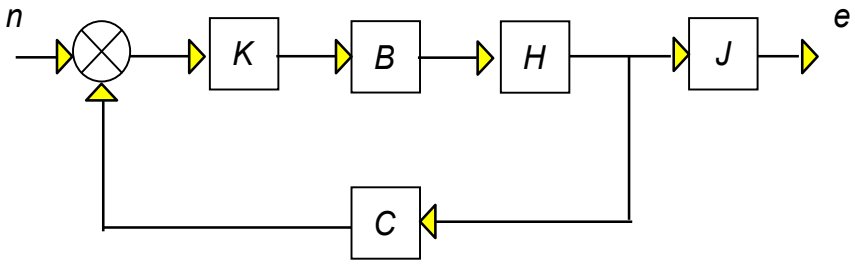

Figure 8. Noise and errors in block diagram form.

Figure 9 illustrates the disturbance for controlling the transfer function:

$$T_{du} = (I - KCHB)^{-1} KCH \cdot G \tag{19}$$

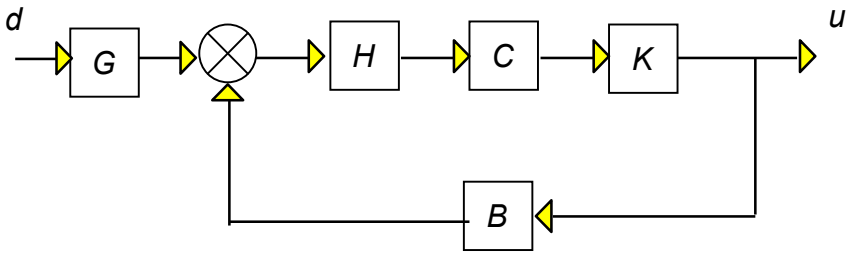

Figure 9. Disturbance and control voltages presented in a block diagram form.

Figure 10 shows that the noise-to-control transfer function is

$$T_{nu} = (I - KCHB)^{-1} K \tag{20}$$

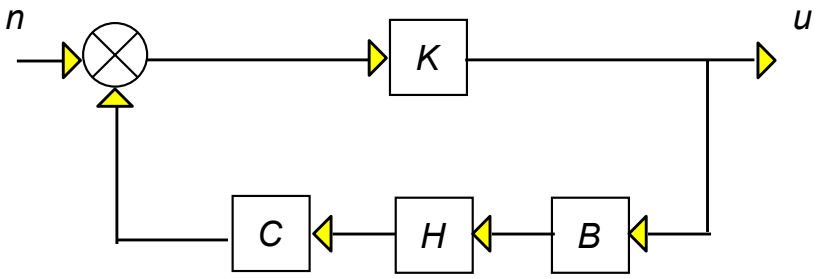

Figure 10. Noise and control voltages presented in a block diagram form.

When we combine these, we obtain

$$e = J \cdot (I - HBKC)^{-1} H \cdot Gd + J \cdot (I - HBKC)^{-1} HBKn \tag{21}$$

$$u = (I - KCHB)^{-1} KCH \cdot Gd + (I - KCHB)^{-1} Kn \tag{22}$$

or

$$\begin{bmatrix} u \\ e \end{bmatrix} = \begin{bmatrix} (I - KCHB)^{-1} KCHG & (I - KCHB)^{-1} K \\ J(I - HBKC)^{-1} HG & J(I - HBKC)^{-1} HBK \end{bmatrix} \begin{bmatrix} d \\ n \end{bmatrix} \tag{23}$$

$$\begin{bmatrix} u \\ e \end{bmatrix} = \begin{bmatrix} F_{du} & F_{nu} \\ F_{de} & F_{ne} \end{bmatrix} \begin{bmatrix} d \\ n \end{bmatrix} \Rightarrow z = F(s)w \tag{24}$$

We proceeded by making the necessary weighting adjustments and redesigning Figure 6 to fit our particular issue.

Next, we created a new version of Figure 11, restructuring it into a two-port diagram. This new diagram should be formatted in a manner similar to that depicted in Figure 6. This comparison will help us better understand the differences and similarities between the two representations.

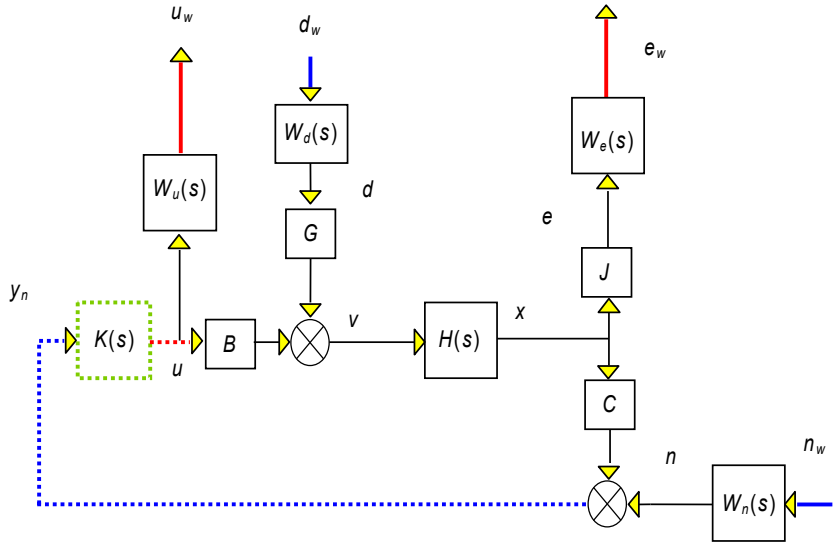

Figure 11. A block diagram showing the beam scenario's weights.

In Figure 12, x and v are auxiliary signals.

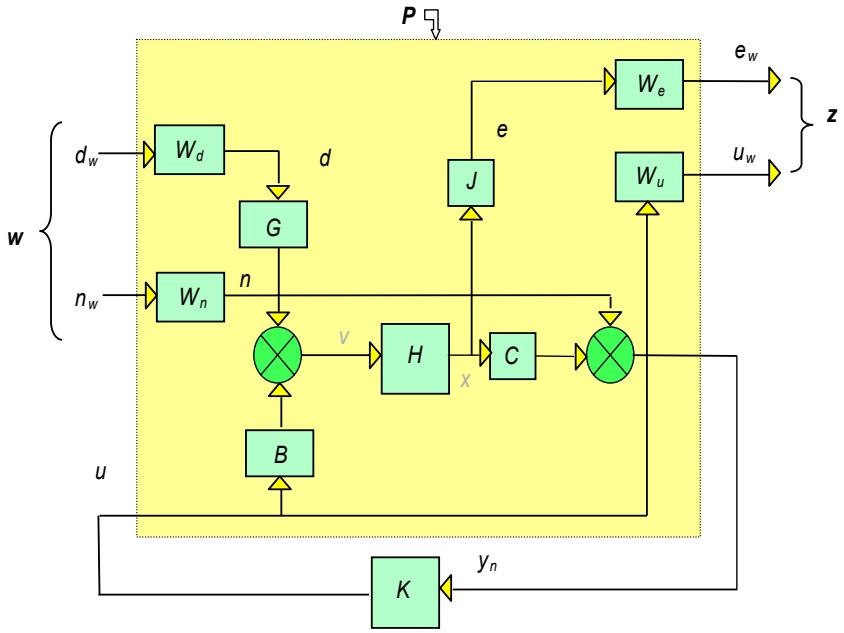

Figure 12. Diagram with two ports for the beam issue.

We were investigating why

$$Q_{zw}(s) = P_{zw}(s) + P_{zu}(s)K(s)\,(I - P_{yu}(s)K(s))^{-1}P_{yw}(s) \tag{25}$$

such that

$$z = Q_{zw}w = F(P, K)w \tag{26}$$

We then attempted to identify P(s). The necessary transfers carried out were

$$ew = WeJx = WeJHv = WeJH(GWddw + Bu) = WeJHGWddw + WeJHBu \quad (27)$$

$$uw = Wuu \quad (28)$$

$$yn = Cx + Wnnw = CHv + Wnnw = CH(GWddw + Bu) + Wnnw = CHGWddw + CHBu + Wnnw \quad (29)$$

Combining all these results in

$$\begin{bmatrix} u_w \\ e_w \\ y_n \end{bmatrix} = \begin{bmatrix} 0 & 0 & W_u \\ W_eJHGW_d & 0 & W_eJHB \\ CHGW_d & W_n & CHB \end{bmatrix} \begin{bmatrix} d_w \\ n_w \\ u \end{bmatrix} \quad (30)$$

or

$$\begin{bmatrix} z \\ y_n \end{bmatrix} = \begin{bmatrix} P_{zw} & P_{zu} \\ P_{yw} & P_{yu} \end{bmatrix} \begin{bmatrix} w \\ u \end{bmatrix} \quad (31)$$

where

$$P_{zw} = \begin{bmatrix} 0 & 0 \\ W_eJHGW_d & 0 \end{bmatrix},\ P_{zu} = \begin{bmatrix} W_u \\ W_eJHB \end{bmatrix},\ P_{yw} = \begin{bmatrix} CHGW_d & W_n \end{bmatrix},\ P_{yu} = CHB \quad (32)$$

However, further steps are required to obtain Qij. To do sp, we used Equation (18), noting that

$$d = W_d d_w,\ n = W_n n_w,\ e_w = W_e e,\ u_w = W_u u$$

Hence,

$$\begin{bmatrix} u \\ e \end{bmatrix} = \begin{bmatrix} W_u^{-1} u_w \\ W_e^{-1} e_w \end{bmatrix} = F(s) \begin{bmatrix} d \\ n \end{bmatrix} = F(s) \begin{bmatrix} W_d d_w \\ W_n n_w \end{bmatrix} \Rightarrow$$
$$\begin{bmatrix} u_w \\ e_w \end{bmatrix} = \begin{bmatrix} W_u & \\ & W_e \end{bmatrix} F(s) \begin{bmatrix} W_d & \\ & W_n \end{bmatrix} \begin{bmatrix} d_w \\ n_w \end{bmatrix}$$

or

$$\begin{bmatrix} u_w \\ e_w \end{bmatrix} = \begin{bmatrix} W_u(I - KCHB)^{-1}KCHGW_d & W_u(I - KCHB)^{-1}KW_n \\ W_eJ(I - HBKC)^{-1}HGW_d & W_eJ(I - HBKC)^{-1}HBKW_n \end{bmatrix} \begin{bmatrix} d_w \\ n_w \end{bmatrix}$$

Thus, the matrices in

$$z = Q_{zw}w \text{ or } \begin{bmatrix} u \\ e \end{bmatrix} = \begin{bmatrix} Q_{11} & Q_{12} \\ Q_{21} & Q_{22} \end{bmatrix} \begin{bmatrix} d \\ n \end{bmatrix}$$

From the natural partitioning to express P in state–space,

$$P(s) = \begin{bmatrix} A & B_1 & B_2 \\ C_1 & D_{11} & D_{12} \\ C_2 & D_{21} & D_{22} \end{bmatrix} = \begin{bmatrix} P_{zw}(s) & P_{zu}(s) \\ P_{yw}(s) & P_{yu}(s) \end{bmatrix} \quad (33)$$

(where the shortened format is used), and K's corresponding form is

$$K(s) = \begin{bmatrix} A_K & B_K \\ C_K & D_K \end{bmatrix}$$

Equation (29) describes the equations

$$\dot{x}(t) = Ax(t) + \begin{bmatrix} B_1 & B_2 \end{bmatrix} \begin{bmatrix} w(t) \\ u(t) \end{bmatrix}$$
$$\begin{bmatrix} z(t) \\ y(t) \end{bmatrix} = \begin{bmatrix} C_1 \\ C_2 \end{bmatrix} x(t) + \begin{bmatrix} D_{11} & D_{12} \\ D_{21} & D_{22} \end{bmatrix} \begin{bmatrix} w(t) \\ u(t) \end{bmatrix}$$

and

$$\dot{x}K(t) = AKxK(t) + BKy(t)$$

$$u(t) = CKxK(t) + DKy(t)$$

3. Results

3.1. H_2 Norm

In the control theory, the H_2 norm or H_2 performance is used to evaluate the performance of a system [6,7,25–27,29,30]. Significantly, it quantifies a system's ability to reduce noise and disturbances by measuring its energy in response to white noise. The H_2 norm of the system is defined by taking the square root of the sum of the squares of the impulse responses. The total system power response to a unit impulse input can be represented by the H_2 norm. It is an indicator of the amount of energy from the input signals that are attenuated or amplified across all frequency intervals by the system. In principle, a lower H_2-norm indicates higher disturbance rejection and noise attenuation capacity. Minimizing the H_2 norm is often a goal in the control system design, particularly in optimal control frameworks. The use of the H_2 criterion for controllers that perform well under different operational circumstances is widespread in practice because it combines performance with robustness [16–21,28].

Controller design in control systems aims to reduce the H_2 norm, particularly in optimal control frameworks. Because it strikes a good balance between robustness and performance, the H_2 standard is a popular choice for controller design that must operate effectively across various operating conditions [16–21,28]. In summary, the H_2 norm of control theory is useful for building systems that work well on average, even with noise and disturbances. Engineers can then reduce the H_2 norm to develop controllers that enhance the overall robustness and energy efficiency of a system [1,6,7,25–27,29–31,35,36].

3.2. H-Infinity Norm

The H∞ (H-infinity) norm is crucial in control theory, particularly when designing robust controls to assess and ensure system performance in worst-case scenarios [11,35,36]. The highest gain that the system can gain from its input to its output at all frequencies is indicated by the H∞ norm. This denotes the amount of noise or disturbance that can be amplified by the system in the worst-case scenario. A lower H∞ norm will practically result in a more robust system because it is unlikely to cause significant damage, even during worst-case situations. Therefore, it is necessary to minimize this norm when designing control systems for robust performance. The H∞ control structure aims to design controllers with good performance despite uncertainties and worst-case disruptions. Systems that require dependability and safety, such as those in aerospace, are where they matter the most [16–21,28].

It is possible to compute the H∞ norm for state–space representations. Describe a system in which y = Cx and $x^{\cdot}$ = Ax + Bu. Solving the algebraic Riccati equation (ARE) for any given PPP matrix and verifying whether the closed-loop system is stable will yield the H∞ norm. The H_2 norm is not equal to H∞ because it calculates the entire energy response of the system to the white noise inputs. The H∞ norm considers the worst-case scenario, whereas H_2 provides an assessment of performance averaged over time. Therefore, the H∞ norm is more appropriate when a high degree of robustness is required [2,11,35,36].

In summary, the H∞ norm plays the most important role in the robust control theory by demonstrating the highest possible amplification of disturbances by a system. Designing controllers that minimize the H∞ norm allows control engineers to guarantee robust stability even under extreme difficulties. The results are then presented in the following format: in the first case, a sinusoidal loading amplitude of 12N was applied, followed by constant loading. The result is a comparison of control H_2 with H∞. Structures apply the H_2 norm or H_2 performance as a measure of performance, as used in control theory. In particular, it measures the power of the system output due to white noise inputs to show how effectively the system can dampen noise and interference.

3.3. H-Infinity and H_2 Norms Comparison

The H_2 norm is dissimilar to the H∞ norm, which is defined as the peak value of the system gain at all frequencies. The H_2 norm averages the energy measure and the H∞ norm concentrates on the maximum response. Depending on the design requirements, control engineers may choose to minimize either H_2 or the H∞ norm.

In practice, the H_2 norm is beneficial for systems where disturbances and noise are random processes with known statistical characteristics. It is especially useful in cases where the ability of an antenna to work in a frequency range is more important than its ability to work at a precise frequency.

The H∞ norm is another form of the norm and is defined as the maximum gain of the system at any frequency. It estimates the phase margin to account for the maximum possible amplification of the disturbances or noise by the system. For a fair comparison, it was necessary to arrange the results to show that a lower H∞ norm better reflects the robustness of the system because the system is less influenced by worst-case disturbances.

One part of the code for H-infinity controller (Figure 13) is

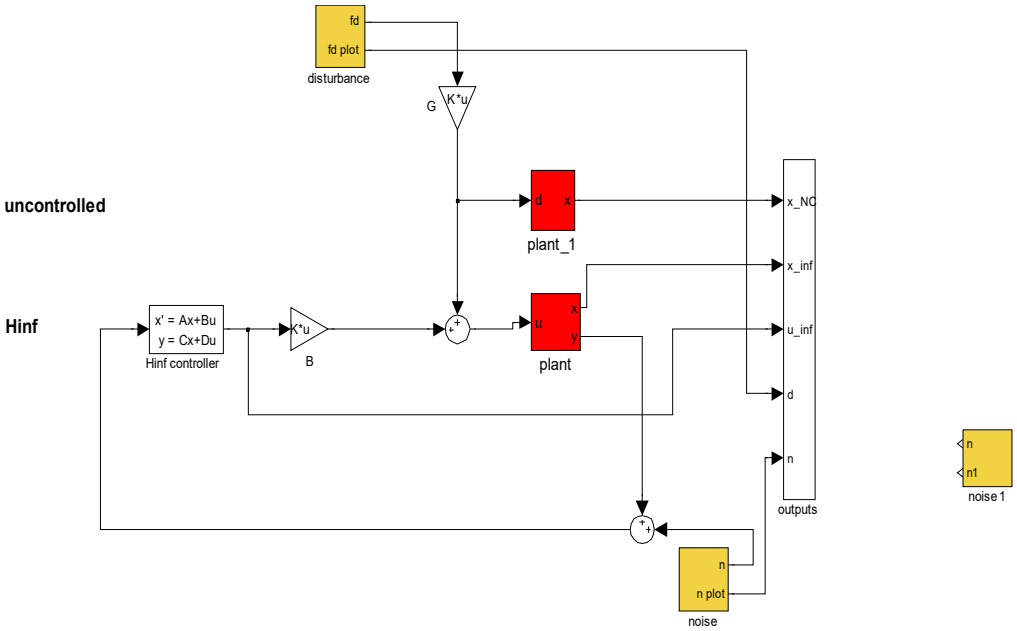

Figure 13. Nominal performance in Simulink, where Wd, Wn, Wu, and We are the whets of our system for disturbances (d) noise (n), control vector (u), and error (e); x is the state vector and y is the output; in the displacement the rotation and the control vector (u), K is our control (H-infinity or H_2). In the results, we take the diagram for the open loop (without control) with H-infinity and the H_2 controller.

```
    AT = A0;
    BT = [Bm0 zeros(2*nd, nd/2) Be0];
    CT = [J; C0];
    DT = [zeros(nd, nd) zeros(nd, nd/2) zeros(nd, nd/2); zeros(nd/2, nd)
eye(nd/2) zeros(nd/2, nd/2)]
    qbeam2 = ss(AT, BT, CT, DT);
    szk = size(Kinf.a, 1);
    [Kinf, Scl12, gam12] = hinfsyn(qbeam2, nmeas, ncont)
    save Kinf.mat Kinf
    return
    % full weight
    systemnames = ' beam0 y sd se su Wu We Wn Wd';
    inputvar = '[ n(4); d(8); u(4) ]';
```

```
outputvar = '[ We; Wu; y+Wn]';
input_to_sd = '[Wd]';
input_to_su = '[u]';
input_to_se = '[beam0]';
input_to_beam0 = '[ sd+su ]';
input_to_y = '[ beam0 ]';
input_to_Wd = '[ d ]';
input_to_Wn = '[ n ]';
input_to_We = '[ se ]';
input_to_Wu = '[ u ]';
return
Kinf
```

3.4. Mathematical Modeling Results

Figures 14 and 15 compare the rotations and translations of the nodes in the smart architectures with and without control, respectively. This analysis highlights the significant impact of the control system. Without control, the nodes exhibited substantial rotational movement, indicating a lack of stability and an increased susceptibility to oscillations. Conversely, the rotations were markedly reduced with the control system in place, demonstrating the effectiveness of the system in enhancing stability and minimizing unwanted movements. This comparison underscores the critical role of the control mechanism in retaining the structural integrity and performance of the smart structures.

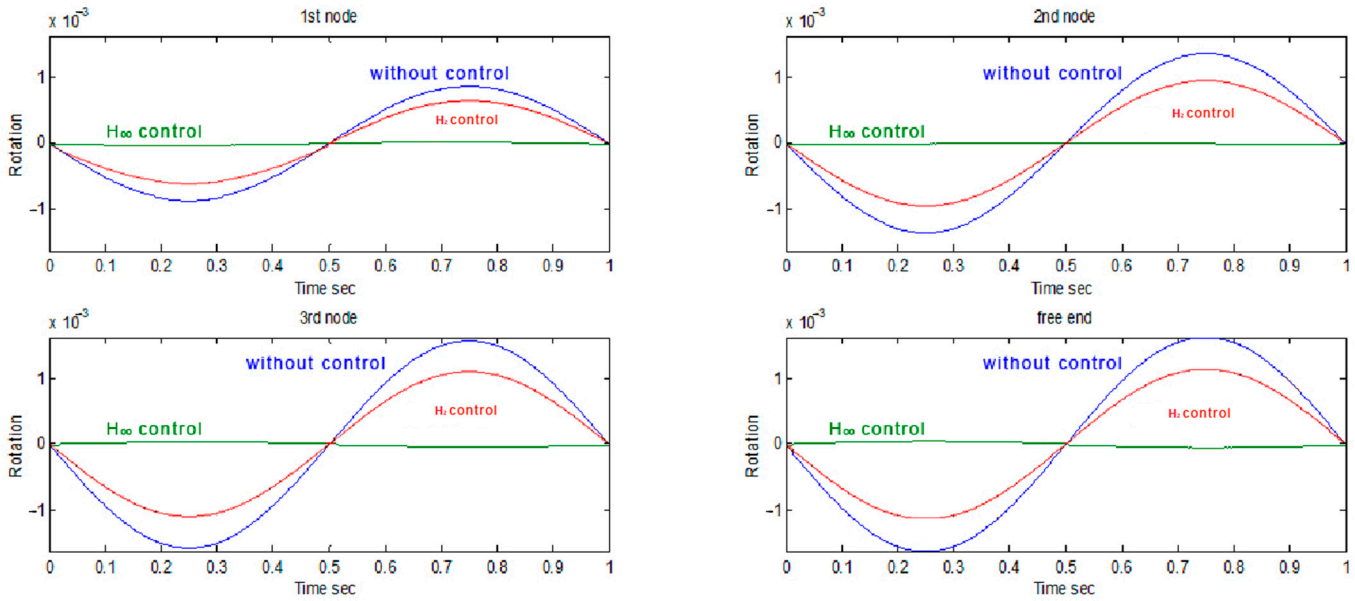

Figure 14. Comparing the nodes' rotations in the smart structures both with and without control.

In Figure 14, the four nodes of the smart structure rotations are depicted for three different scenarios: with H_2 control, H∞ (H-infinity) control, and without any control. The results clearly show that H∞ control provides the best performance, as the rotations are nearly zero. This indicates that the H∞ control method is highly effective in minimizing rotational movement systems [1,6,7,11,25–27,29–31,35].

Similarly, Figure 15 illustrates the displacements of the four smart structure nodes under the same three scenarios: with H_2 control, with H∞ control, and without control. The comparison reveals that H∞ control yields a superior outcome. The displacements were almost zero when the H∞ control was applied, demonstrating its effectiveness in minimizing positional deviations. Thus, the H∞ control proved to be the most effective method for reducing both rotations and displacements in smart structures.

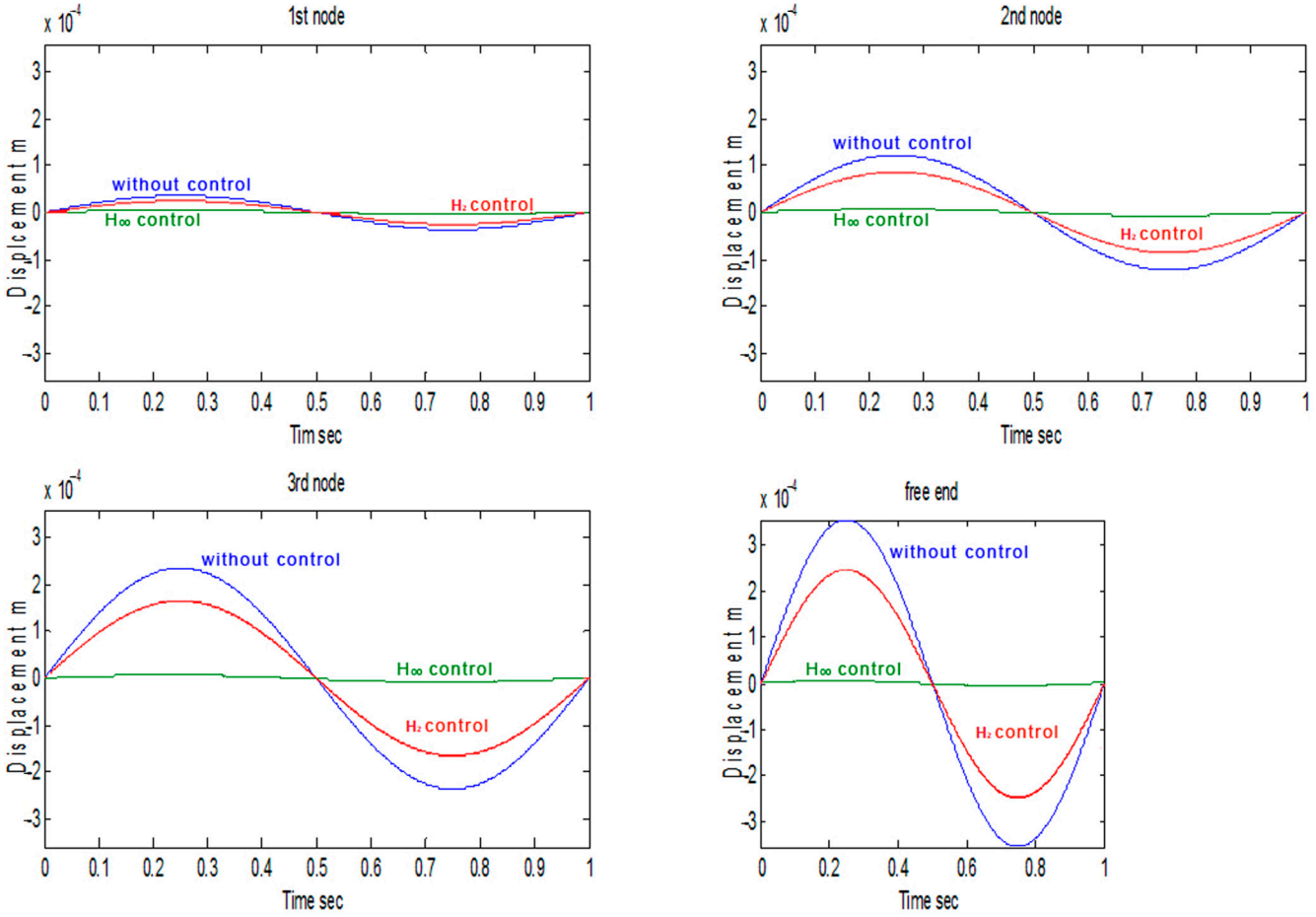

Figure 15. Analyzing and contrasting the smart structure node displacements with and without control.

The results are then provided in detail for the static loading of 12 N at the free end of the smart structure. In Figures 16–18, a concentrated force (12N) is applied to the edge of the carrier, and the displacement at the edge of the carrier quickly stabilizes at 0.015 sec. This shows the very good operation of the model. In addition, what is also the goal of the specific problem is achieved, i.e., a reduction in oscillation since with the blue line, we have a result with control where I is a reduction in distortion, while with the green line, I is the open loop in which the oscillation is much greater.

Figure 16 illustrates the displacements for all the nodes of the smart beam, where the H-infinity control criterion is employed. The results are highly impressive because the displacements were negligible. This illustrates how the H-infinity control strategy effectively reduces the displacements while maintaining the stability and structural integrity of the smart beam under static loading scenarios. The near-zero displacement highlights the superior performance and robustness of the control system [6,7,26,30,31].

Figure 17 depicts the rotations for all the nodes of the smart beam using the H-infinity control criterion. The findings were exceptionally impressive as the displacements were nearly imperceptible. This underscores the efficacy of the H-infinity control approach in reducing displacements to a minimum, thereby ensuring the structural integrity and stability of the smart beam under static loading scenarios. The minimal rotations for all the nodes of the smart beam highlight the superior performance and robustness of the implemented control system.

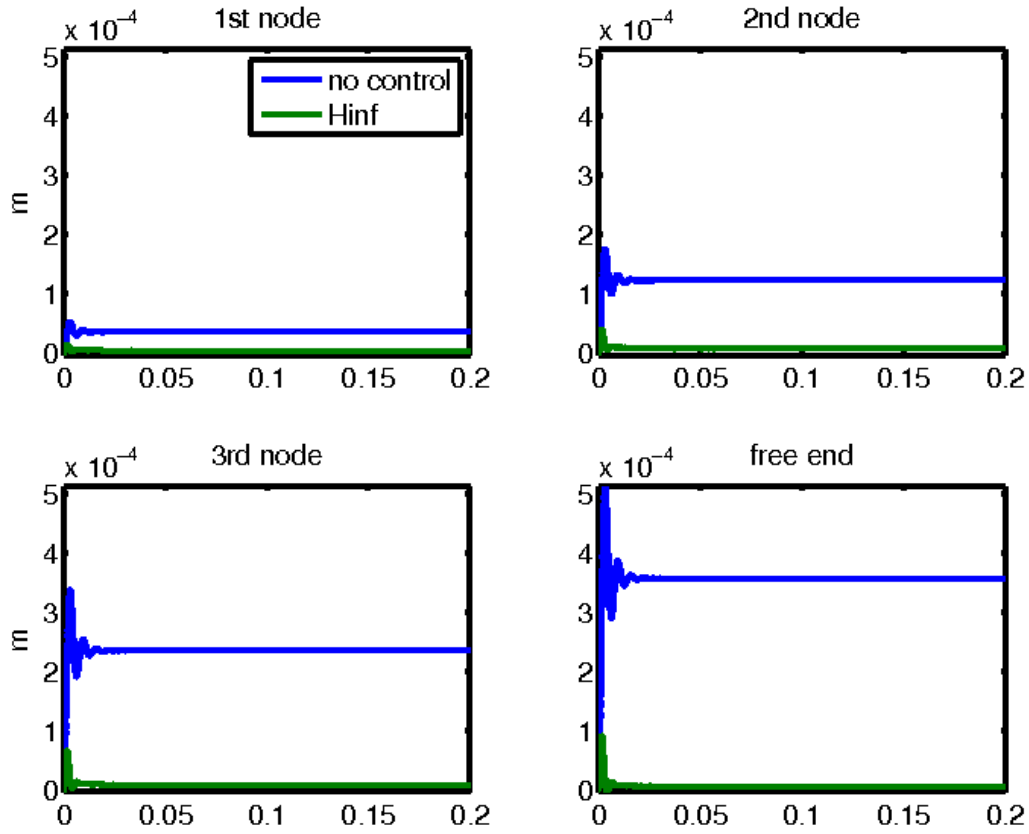

Figure 16. Results of displacements with and without control when applying static loading at the beam's free end.

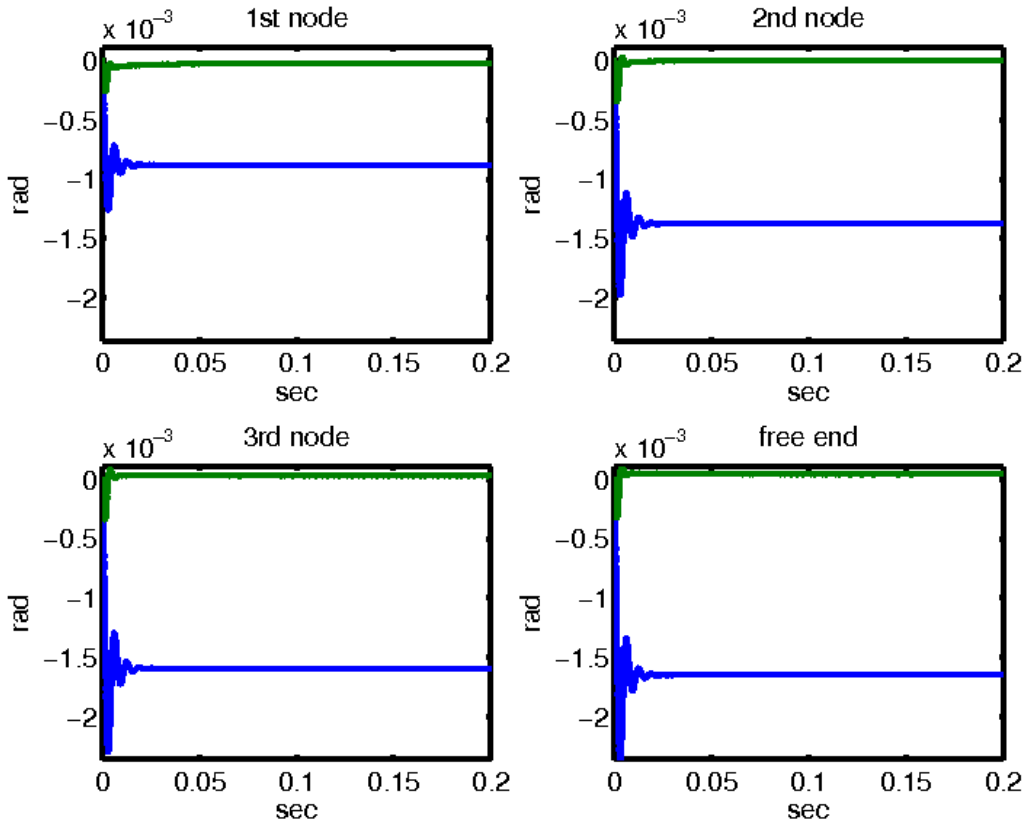

Figure 17. Results of rotations with and without control when applying static loading at the beam's free end.

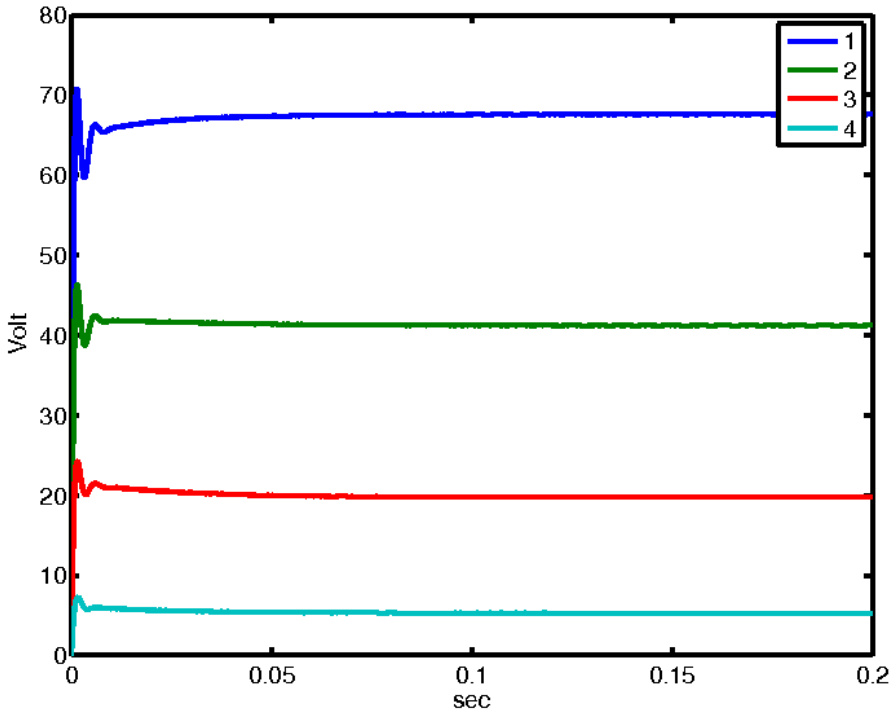

Figure 18. Control voltages for each smart structure node. The numbers 1, 2, 3, and 4 correspond to the four piezoelectric actuators (voltages) present in the smart beam.

The results for the four smart beam nodes are shown in Figure 18. This figure shows the piezoelectric stresses produced, which are necessary for damping oscillations. The data provided a clear insight into how piezoelectric elements contribute to reducing vibrational movement, highlighting the effectiveness of the smart beam design in mitigating oscillatory behavior through targeted stress generation.

Next, sinusoidal loading was applied while utilizing the H-infinity control theory. The results are highly impressive, as there is a noticeable reduction in oscillations. Figure 19 shows the displacement of the structural free end with and without the installed control system. These findings were remarkable, showing a complete reduction in oscillations when the control system was implemented. This highlights the efficacy of the H-infinity control theory in managing and mitigating vibrational movements and ensuring the structural stability and performance of smart structures under sinusoidal loading conditions. A comparison between the controlled and uncontrolled scenarios underscores the significant impact of the control mechanism on achieving optimal structural behavior. Figure 20 shows the displacement of the 3rd node of the structure with and without the control system. The results are remarkable, revealing the complete elimination of oscillations when the control system is active. This underscores the efficacy of the H-infinity control theory in reducing vibrational movements and ensuring the performance and stability of the smart structure under sinusoidal loading conditions. The comparison between controlled and uncontrolled scenarios highlights the crucial role of the control mechanism in optimizing the structural behavior. The control voltages under sinusoidal disturbances for all the nodes of the smart structures are shown in Figure 21. These voltages are crucial for counteracting disturbances and maintaining structural stability. By applying these control voltages, the system effectively mitigates the impact of sinusoidal disturbances, ensuring optimal performance and reducing oscillatory behavior in smart structures. A detailed analysis of these control voltages highlights their significance in achieving precise and efficient control over structural responses. Figure 21 shows the generated piezoelectric stresses, which are essential for damping oscillations. The data offer a clear understanding of how piezoelectric elements help reduce vibrational movement, emphasizing the effectiveness of smart beam design in mitigating oscillatory behavior through precise stress generation.

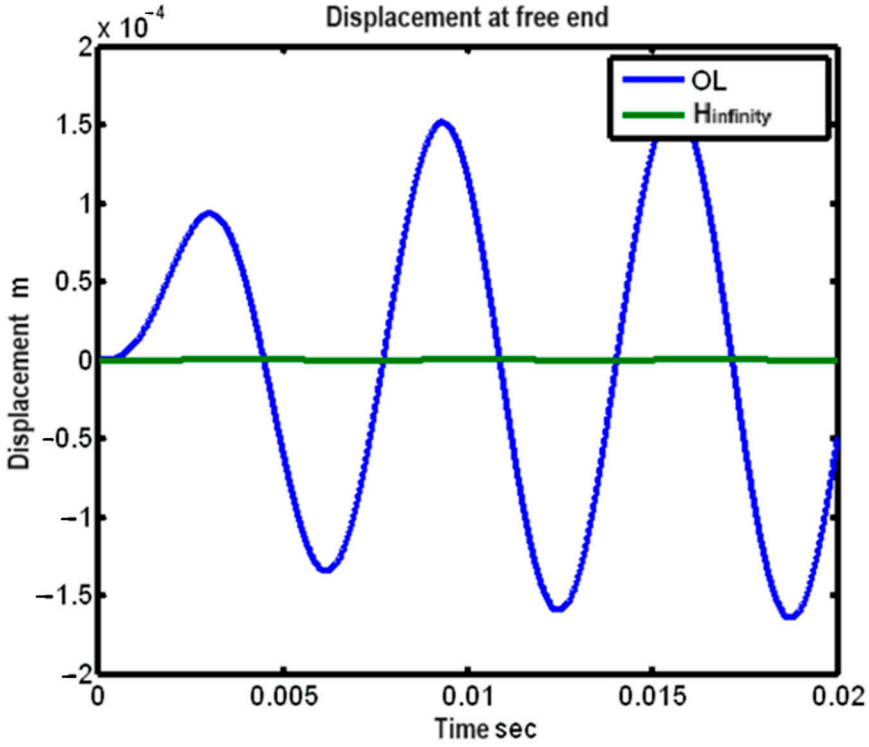

Figure 19. Smart structure's free end displacement with (H-infinity) and without control (open loop, OL).

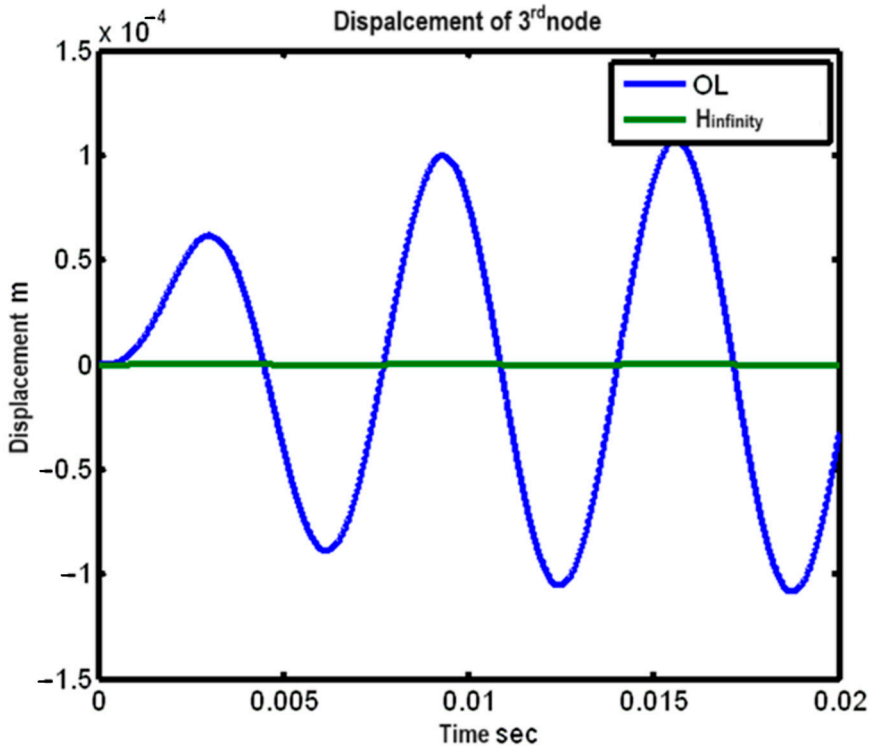

Figure 20. Displacement of the 3rd node of the smart structure presented with (H-infinity) and without control (open loop, OL).

Figure 22 presents a Bode diagram of the smart structure, which illustrates the frequency response of the system. This diagram provides critical insight into the gain and phase shift of a smart structure over a range of frequencies. By analyzing the Bode diagram, one can assess the performance and stability of the control system and identify how effectively it mitigates disturbances and responds to various frequencies. The Bode plot

highlights key characteristics such as resonant frequencies and bandwidths, which are essential for understanding and optimizing the dynamic behavior of a smart structure.

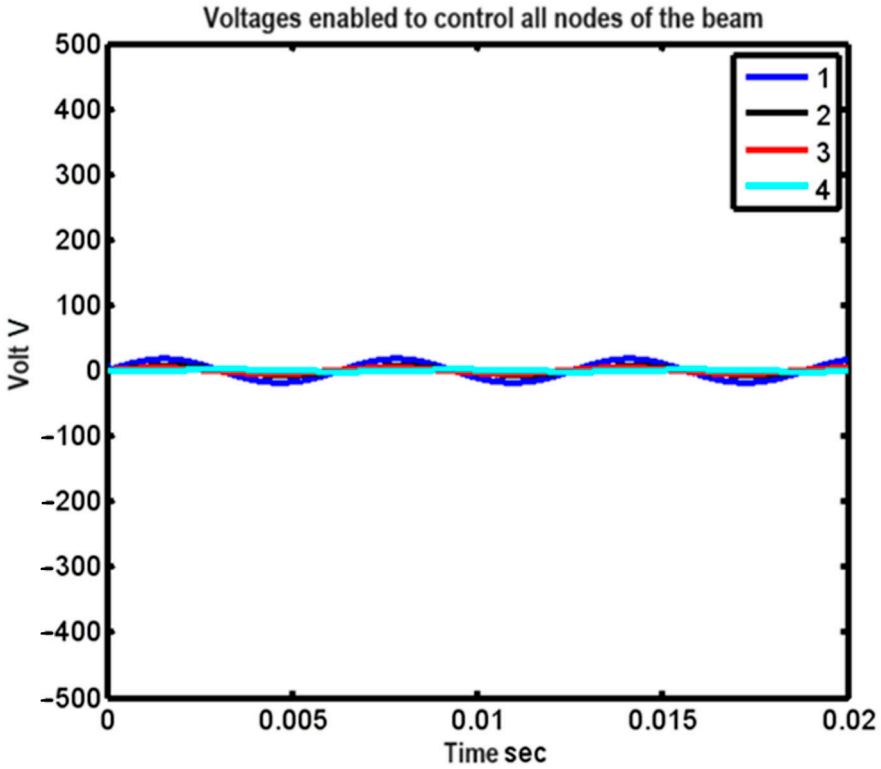

Figure 21. Control voltages for all the nodes of the smart structures under sinusoidal disturbances. The numbers 1, 2, 3, and 4 correspond to the four piezoelectric actuators (voltages) present in the smart beam.

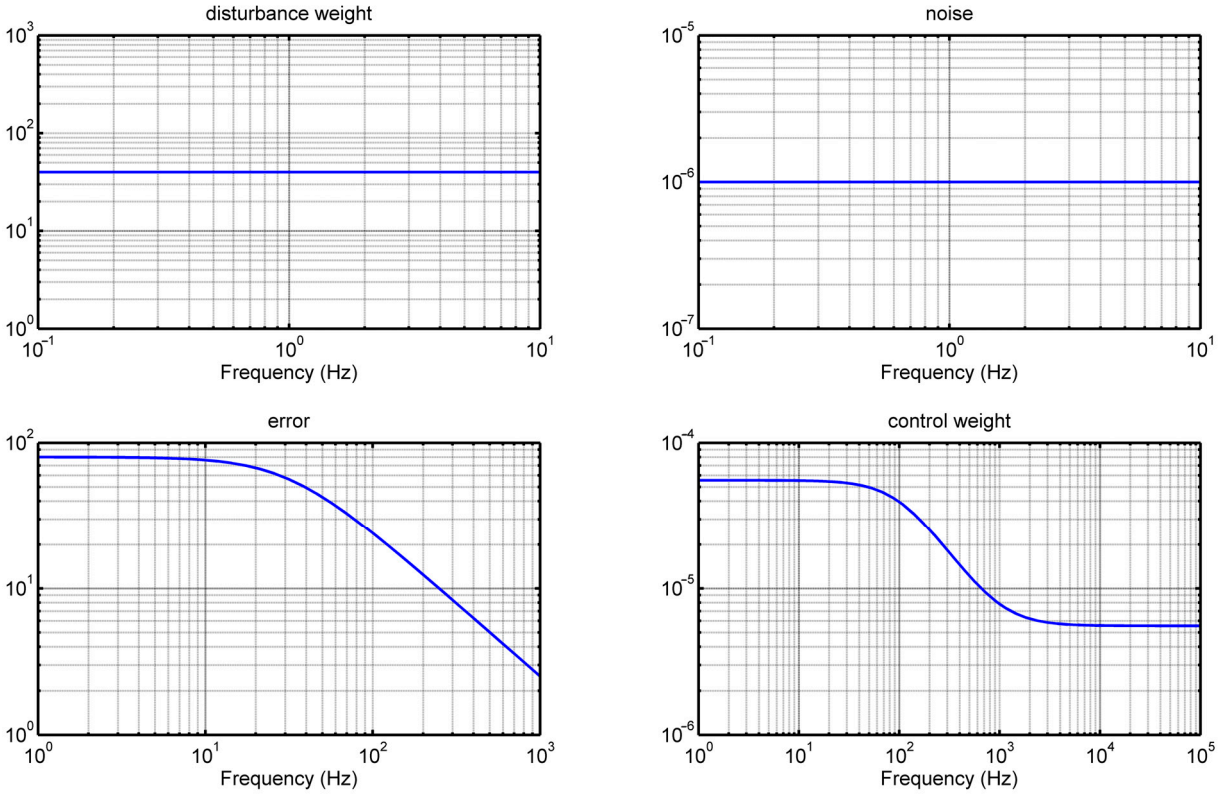

Figure 22. The Bode diagram of the smart structures. ϒ axis is the magnitude (dB).

4. Discussion

This approach employs intelligent control techniques with a robust controller that minimizes the oscillations. Thus, a review of the parameters and their utilization in enhancing the system efficiency, as well as the system survey used to determine the crash resilience of the system. Considerable importance is attached to the disturbance rejection of smart structures that incorporate piezoelectric materials. This work contributes significantly to the reduction in oscillations. The initial modeling was performed using the finite element method. Subsequently, the equations for control theory are given. Equations (1)–(10) aid in the computation of the matrices for mass, damping, and stiffness as well as the matrices input to the electric charge matrix because of the piezoelectric patches.

All registers were calculated by the authors. Both state–space domain analysis Equations (10)–(14) and frequency domain analysis Equations (15)–(33) were used. The results first show us the comparison of the two controllers. Initially, both controllers should make a reduction in the oscillations in relation to the results without control (this is carried out by both). The two controllers are then compared to each other to see which achieves the greatest reduction.

By combining the H-infinity and H_2 methods within the simulated state–space and the frequency of characterization, this study examined the benefit of resilient control in intelligent systems. This study proposes a step-by-step method for generating and implementing stable controllers that are acceptable for intelligent structures. It proposes a robust approach for structural identification by strong control and deals with a state–space model and the frequency domain constructed from the output and input data of the structure. A controller for reducing vibrations is created using this control paradigm. The main concern of the theory is to control the variability of the system behavior. Vibration control techniques have been applied to minimize vibrations through dynamic disturbances, which are vital in mechanical systems, where operations might occur under stochastic loading scenarios. In this study, oscillations were completely suppressed, which was not achieved in earlier studies. In this work, two control techniques to suppress oscillations are employed, and a comparison is made. The results are good in both the frequency and state spaces. All calculations were performed with great accuracy owing to the optimized intelligent control systems. Although this topic has been discussed by several academics [1–3,11,35,36], the current study's findings are superior to those of prior research [2–4,14,33,36].

The advantages of this work include the following: MATLAB was used to program and manipulate the measurement noise from the beam condition to obtain the above results. The total oscillations were suppressed and simultaneously, the order of the controller was reduced. White noise was applied as the disturbance input, and its amplitude was described in terms of disturbances. This is aimed at the development of reliable controllers for smart structures with piezoelectric materials to address ambiguity and improve disturbance rejection. This study delves into the various methods and control techniques used to address this issue and provides a comprehensive description and analysis. The findings of this work hold substantial importance as they offer practical solutions to the widespread problem of oscillation reduction, which is a common concern in both the civil and mechanical engineering disciplines. The applications of this research are far-reaching, with potential uses in the stabilization of airplanes, metal bridges, and large metals. It should be noted that MATLAB codes are written by the article authors, and no code is off-the-shelf or taken from elsewhere. The finite element theory and advanced control theory were used. Initially, it was applied to a beam because the computational requirements for this model with infinite control are very large.

5. Conclusions

This study combined H_2 and H-infinity control to achieve complete vibration reduction in intelligent structures. Specifically, in vibration suppression applications, the resilience of the H-infinity controller to parametric uncertainty is emphasized. This study

provides an excellent example of the benefits of active vibration suppression and robust control in the dynamics of intelligent structures. H-infinity control considers the modeling uncertainties that are difficult to introduce using different techniques. To do this, we used advanced programs written by the authors. The novelty of our work lies in the application of the H-infinity control theory specifically for oscillation damping, combined with its implementation using the finite element method. In our work, we managed to fully suppress the oscillations using the controller H-infinity. The piezoelectric material was inserted along the entire length of the beam. Reliable control systems can benefit from the many advantages of H-infinity control, which minimizes oscillations even when actuator placements vary. Numerical modeling validates that the suggested techniques are successful in lowering vibrations in piezoelectric smart structures. Herein, the benefits of robust control in intelligent structures are explored through the application of H-infinity regulation in both state and frequency domains.

The following are the key aspects of this work:

1. H_2 and H-infinity control are combined to achieve comprehensive vibration reduction in smart structures.
2. Demonstrating the resistance of H-infinity control to parametric uncertainties.
3. Highlighting the benefits of robust control and active vibration suppression in intelligent structures.
4. Showing that H-infinity control can minimize oscillations regardless of actuator placement.
5. Validating the effectiveness of the proposed vibration reduction methods through numerical modeling.
6. H-infinity regulation was used to investigate the advantages of strong control in intelligent structures in both state and frequency domains.
7. Results in the frequency domain and time–space domain: The study presents results in both the frequency domain and time–space domain, providing a comprehensive understanding of the system's dynamic behavior and control performance.

This study significantly advances the understanding and application of control methods in intelligent structures, thereby demonstrating the effectiveness of robust control techniques. In our research, we successfully managed to fully eliminate oscillations by employing the H-infinity control method. To achieve this, we incorporated piezoelectric elements along the entire beam length to ensure comprehensive coverage for optimal control. The modeling and simulation of the system were performed using custom codes, specifically compiled and developed by the authors, to accurately represent the dynamics of the system. A detailed description of the experimental setup, as well as the outcomes of the physical tests, will be presented in future work and publications.

Author Contributions: A.M. and M.P.: software, formal analysis, writing review, and editing; G.E.S.: methodology; A.P.: investigation and software; N.V.: validation. All authors have read and agreed to the published version of the manuscript.

Funding: This research received no external funding.

Data Availability Statement: The data presented in this study are available upon request from the corresponding author.

Acknowledgments: The authors are grateful for the support from the Hellenic Mediterranean University and the Technical University of Crete.

Conflicts of Interest: The authors declare no conflicts of interest.

References

1. Benjeddou, A.; Trindade, M.A.; Ohayon, R. New Shear Actuated Smart Structure Beam Finite Element. *AIAA J.* **1999**, *37*, 378–383. [CrossRef]
2. Bona, B.; Indri, M.; Tornambe, A. Flexible Piezoelectric Structures-Approximate Motion equations and Control Algorithms. *IEEE Trans. Autom. Control* **1997**, *42*, 94–101. [CrossRef]

3. Okko, B.; Kwakernaak, H.; Gjerrit, M. *Design Methods for Control Systems*; Course Notes, Dutch Institute for Systems and Control; Dutch Institute of Systems and Control: Delft, The Netherlands, 2001; Volume 67.
4. Burke, J.V.; Henrion, D.; Lewis, A.S.; Overton, M.L. Hifoo—A MATLAB Package for Fixed-Order Controller Design and H∞ Optimization. *IFAC Proc. Vol.* **2006**, *39*, 339–344. [CrossRef]
5. Yang, S.M.; Lee, Y.J. Optimization of Noncollocated Sensor/Actuator Location and Feedback Gain in Control Systems. *Smart Mater. Struct.* **1993**, *2*, 96. [CrossRef]
6. Ramesh Kumar, K.; Narayanan, S. Active Vibration Control of Beams with Optimal Placement of Piezoelectric Sensor/Actuator Pairs. *Smart Mater. Struct.* **2008**, *17*, 55008. [CrossRef]
7. Hanagud, S.; Obal, M.W.; Calise, A.J. Optimal Vibration Control by the Use of Piezoceramic Sensors and Actuators. *J. Guid. Control Dyn.* **1992**, *15*, 1199–1206. [CrossRef]
8. Song, G.; Sethi, V.; Li, H.-N. Vibration Control of Civil Structures Using Piezoceramic Smart Materials: A Review. *Eng. Struct.* **2006**, *28*, 1513–1524. [CrossRef]
9. Miara, B.; Stavroulakis, G.; Valente, V. Topics of Mathematics for Smart Systems. In Proceedings of the European Conference, Rome, Italy, 26–28 October 2006.
10. Karatzas, I.; Lehoczky, J.P.; Shreve, S.E.; Xu, G.-L. *Modeling, Control and Implementation of Smart Structures: A FEM-State Space Approach*; Springer: Berlin/Heidelberg, Germany, 1990; ISBN 9783540483939.
11. Moutsopoulou, A.; Stavroulakis, G.E.; Pouliezos, A.; Petousis, M.; Vidakis, N. Robust Control and Active Vibration Suppression in Dynamics of Smart Systems. *Inventions* **2023**, *8*, 47. [CrossRef]
12. Zhang, N.; Kirpitchenko, I. Modeling Dynamics of A Continuous Structure with a Piezoelectric Sensoractuator for Passive Structural Control. *J. Sound. Vib.* **2002**, *249*, 251–261. [CrossRef]
13. Zhang, X.; Shao, C.; Li, S.; Xu, D.; Erdman, A.G. Robust H∞ Vibration Control for Flexible Linkage Mechanism Systems with Piezoelectric Sensors and Actuators. *J. Sound. Vib.* **2001**, *243*, 145–155. [CrossRef]
14. Packard, A.; Doyle, J.; Balas, G. Linear, Multivariable Robust Control with a μ Perspective. *J. Dyn. Syst. Meas. Control* **1993**, *115*, 426–438. [CrossRef]
15. Stavroulakis, G.E.; Foutsitzi, G.; Hadjigeorgiou, E.; Marinova, D.; Baniotopoulos, C.C. Design and Robust Optimal Control of Smart Beams with Application on Vibrations Suppression. *Adv. Eng. Softw.* **2005**, *36*, 806–813. [CrossRef]
16. Chandrashekhara, K.; Varadarajan, S. Adaptive Shape Control of Composite Beams with Piezoelectric Actuators. *J. Intell. Mater. Syst. Struct.* **1997**, *8*, 112–124. [CrossRef]
17. Burke, J.V.; Henrion, D.; Lewis, A.S.; Overton, M.L. Stabilization via Nonsmooth, Nonconvex Optimization. *IEEE Trans. Autom. Control* **2006**, *51*, 1760–1769. [CrossRef]
18. Burke, J.V.; Lewis, A.S.; Overton, M.L. A Robust Gradient Sampling Algorithm for Nonsmooth, Nonconvex Optimization. *SIAM J. Optim.* **2005**, *15*, 751–779. [CrossRef]
19. Choi, S.-B.; Cheong, C.-C.; Lee, C.-H. Position Tracking Control of a Smart Flexible Structure Featuring a Piezofilm Actuator. *J. Guid. Control Dyn.* **1996**, *19*, 1364–1369. [CrossRef]
20. Culshaw, B. Smart Structures—A Concept or a Reality. *Proc. Inst. Mech. Eng. Part I J. Syst. Control Eng.* **1992**, *206*, 1–8. [CrossRef]
21. Tzou, H.S.; Gabbert, U. Structronics—A New Discipline and Its Challenging Issues. *Fortschr. -Berichte VDI Smart Mech. Syst.—Adapt. Reihe* **1997**, *11*, 245–250.
22. Zhou, K.; Doyle, J.C.; Glover, K. *Robust and Optimal Control*; Feher/Prentice Hall Digital and Wireless Communication Series; Prentice Hall: Saddle River, NJ, USA, 1996; ISBN 9780134565675.
23. Skogestad, S.; Postlethwaite, I. *Multivariable Feedback Control: Analysis and Design*, 2nd ed.; John Wiley and Sons Ltd., Ed.: Chichester, UK, 2005; ISBN 0-470-01167-X.
24. Doyle, J.C.; Francis, B.A.; Tannenbaum, A. *Feedback Control Theory*; Macmillan Publishing Company: New York, NY, USA, 1992; ISBN 9780023300110.
25. Guran, A.; Tzou, H.-S.; Anderson, G.L.; Natori, M.; Gabbert, U.; Tani, J.; Breitbach, E. *Structronic Systems: Smart Structures, Devices and Systems*; World Scientific: Singapore, 1998; Volume 4, ISBN 978-981-02-2652-7.
26. Tzou, H.S.; Anderson, G.L. *Intelligent Structural Systems*; Springer: Dordrecht, The Netherlands, 1992; ISBN 978-94-017-1903-2.
27. Gabbert, U.; Tzou, H.S. IUTAM Symposium on Smart Structures and Structronic Systems. In Proceedings of the IUTAM Symposium, Magdeburg, Germany, 26–29 September 2000; Kluwer: Dordrecht, The Netherlands, 2001.
28. Tzou, H.S.; Natori, M.C. *Piezoelectric Materials and Continua*; Braun, S.B.T.-E.V., Ed.; Elsevier: Oxford, UK, 2001; pp. 1011–1018. ISBN 978-0-12-227085-7.
29. *Walter Guyton Cady Piezoelectricity: An Introduction to the Theory and Applications of Electromechanical Phenomena in Crystals*; Dover Publication: New York, NY, USA, 1964.
30. Tzou, H.S.; Bao, Y. A Theory on Anisotropic Piezothermoelastic Shell Laminates with Sensor/Actuator Applications. *J. Sound. Vib.* **1995**, *184*, 453–473. [CrossRef]
31. Moutsopoulou, A.; Stavroulakis, G.E.; Petousis, M.; Vidakis, N.; Pouliezos, A. Smart Structures Innovations Using Robust Control Methods. *Appl. Mech.* **2023**, *4*, 856–869. [CrossRef]
32. Cen, S.; Soh, A.-K.; Long, Y.-Q.; Yao, Z.-H. A New 4-Node Quadrilateral FE Model with Variable Electrical Degrees of Freedom for the Analysis of Piezoelectric Laminated Composite Plates. *Compos. Struct.* **2002**, *58*, 583–599. [CrossRef]
33. Kwakernaak, H. Robust Control and H∞-Optimization—Tutorial Paper. *Automatica* **1993**, *29*, 255–273. [CrossRef]

34. Blondel, V.D.; Tsitsiklis, J.N. A Survey of Computational Complexity Results in Systems and Control. *Automatica* **2000**, *36*, 1249–1274. [CrossRef]
35. Bandyopadhyay, B.; Manjunath, T.C.; Umapathy, M. *Modeling, Control and Implementation of Smart Structures A FEM-State Space Approach*; Springer: Berlin/Heidelberg, Germany, 2007; ISBN 978-3-540-48393-9.
36. Kimura, H. Robust Stabilizability for a Class of Transfer Functions. *IEEE Trans. Autom. Control* **1984**, *29*, 788–793. [CrossRef]